The influence of axial compression on the free vibration frequencies of cross-ply laminated and moderately thick cylinders

Eksenel basıncın dik-katmanlı ve orta kalınlıkta silindirlerin serbest titreşim frekanslarına etkisi

Yazar(lar) (Author(s)): İzzet Ufuk ÇAĞDAŞ

ORCID: 0000-0002-2528-2978

Eksenel Basıncın Dik-katmanlı ve Orta Kalınlıkta Silindirlerin Serbest Titreşim Frekanslarına Etkisi

Araştırma Makalesi / Research Article

İzzet Ufuk ÇAĞDAŞ*

Mühendislik Fakültesi, İnşaat Müh. Bölümü, Akdeniz Üniversitesi, Antalya, Türkiye

ÖZ

Bu çalışmada, eksenel basınç altındaki dik-katmanlı kompozit silindirlerin serbest titreşim davranışları dönel atalet ve kalınlık/yarıçap oranını içeren birinci mertebeden uygun bir kayma deformasyonlu kabuk teorisine dayanan yarı-analitik bir sonlu eleman kullanılarak araştırılmıştır. Öncelikle, eksenel simetrik kabuk sonlu elemanının doğrulanması için bir çalışma yapılmış ve basıncın bulunmadığı haller için geliştirilmiş sonlu eleman ile elde edilmiş titreşim frekanslarının literatürde bulunan neticeler ile çok iyi uyum içinde olduğu görülmüştür. Aynı eleman ilk katman göçme analizi için de doğrulanmış ve kayma deformasyonlu bir eğri kabuk elemanı ile ile elde edilen ilk katman göçme yükleri ile iyi uyum gözlenmiştir. Daha sonra, çeşitli sınır şartlarına sahip ve burkulma ve ilk katman göçme yüklerinden düşük olacak şekilde farklı düzeylerde eksenel basınca maruz kompozit silindirler için serbest titreşim analizleri yapılmıştır. Göz önünde bulundurulan silindirik yapıların temel titreşim frekanslarında karşı gelen burkulma yüklerinin % 60 ila 80 nispetinde eksenel yük değerleri için hızla azaldığı gözlemlenmiştir. Ayrıca, bazı nispeten kalın silindirlerde ilk-katman göçme yükünün burkulma yükünden az olduğu da belirlenmiştir.

Anahtar Kelimeler: Titreşim, burkulma, kompozit silindir, sonlu elemanlar, basınç.

The Influence of Axial Compression on the Free Vibration Frequencies of Cross-ply Laminated and Moderately Thick Cylinders

ABSTRACT

In this study, the free vibration behavior of axially compressed cross-ply laminated composite cylinders is investigated using a semi-analytical shell finite element based on a consistent first order shear deformable shell theory, which includes the influences of rotatory inertia and thickness coordinate/radius ratio. First, a verification study is conducted to validate the axisymmetric shell finite element used in this study and, for the non-compressed cases, the free vibration frequencies obtained using the finite element developed are found out to be in excellent agreement with the published results found in the literature. The same element is also validated for first-ply failure analysis and good agreement is observed with the first-ply failure loads obtained using a shear deformable and curved shell element. Then, numerical results for free vibration analyses are presented for axially compressed composite cylinders having different boundary conditions and for which the level of axial compression is kept below the corresponding linear buckling and first ply failure loads. It is observed that, the fundamental free vibration frequencies decrease sharply for axial load levels higher than about 60~80% of the buckling loads of the cylindrical structures considered. It is also determined that the first-ply failure load is lower than the buckling load for some of the thicker cylinders.

Keywords: Vibration, buckling, composite cylinder, finite elements, compression.

1. INTRODUCTION

In the present study, the influence of axial compression on the vibration behavior of cross-ply laminated and moderately cylinders is numerically investigated. The primary aim here is to determine the relationship between the natural frequencies of vibration and buckling in order to be able to predict the onset of buckling.

Surveys on the dynamics of cylindrical shells can be found in the review papers of Qatu [1] and Khdeir et al. [2] and the research study of Jones et al. [3]. The influence of axial loading for homogeneous isotropic, and orthotropic cylindrical shells was treated in several research studies found in the literature [4-13]. Armenàkas [4] has investigated the influence of axial stress on the frequncy of vibration of simply supported circular cylindrical shells using a bending theory. Rosen and Singer [5] have considered stiffened shells under axial compression and have presented analytical results for vibration frequency in comparison with experimental results. Bradford and Dong [6] and Greenberg and Stavsky [7] have investigated the vibratory characteristics of initially stressed laminated orthotropic cylinders. Yamada et al. [8] have investigated simply supported orthotropic cylinders under axial loads using the transfer matrix method. Chang and Lin [9] have considered simply supported and cross-ply laminated thin cylinders and have obtained a closed form solution. Greenberg and Stavsky [10] have also considered the

*Sorumlu Yazar (Corresponding author)
e-posta : izzetufuk@gmail.com

influence of nonuniform axial loads on the vibration characteristics of orthotropic composite cylindrical shells using a complex finite Fourier transform method. Matsunaga [11] has studied the free vibration behavior of thick circular cylinders using a higher order shell theory. Skusis *et al.* [12] have studied the vibration bahevior of steel cylinders under axial compressive loads in a more recent study. Arbelo *et al.* [13] have used experimental results to determine the real boundary conditions of flat plates and cylindrical shells. However, in general, thinner composite cylinders have been studied and the first-ply failure (FPF) load, the thickness coordinate/radius ratio, and different boundary conditions taken into account here, has not been considered in these cited studies. In some of the related studies correlation of Matsunaga [11] has stated that the critical buckling stress of simply supported circular cylindrical shells subjected to initial axial stress can be predicted from the natural frequency of the shell without axial stress. Similar vibration-buckling correlation studies exist in the literature [12, 13].

The finite element numerical results are obtained here using a semi-analytical finite element, which is based on this consistent shell theory developed by Qatu [14], who obtained very accurate free vibration results for laminated composite shells by using a consistent first order shear deformable shell theory. In this theory, the 1+z/R term is taken into account, where z and R denote the thickness coordinate and the radius, respectively. Using the same shell theory, Cagdas [15] has developed a curved axi-symmetric shell element, which is modified here for free vibration analysis, and Cagdas and Adali [16] have investigated the influence of pressure stiffness on the stability of cross-ply laminated moderately thick cylinders under hydrostatic pressure. In more recent studies, Cagdas [17, 18] has modified the same element for the stability and stress analysis of filament wound cones. This study is the first application of this moderately thick shell finite element to composite cylinder vibration problems including compressive loads. Also different boundary conditions are considered in this study.

In order to validate the computer code developed for free vibration analysis, comparisons with published results in the literature are made and excellent agreement with the references for non-compressed cases is observed. Also, the element is validated for FPF analysis by comparing the FPF loads obtained with the ones obtained using a 2D superparametric shell element, developed recently by Cagdas and Adali [19]. After validating the finite element developed, the influence of axial compression on the free vibration frequencies of cross-ply laminated perfect cylinders having different boundary conditions is investigated. Numerical results are presented for axial compression levels less than the corresponding linear buckling or FPF loads of the cylinders. The influences of axial compression on the vibration frequencies are demonstrated by tables and graphs. Moreover, the influence of the boundary conditions are investigated.

2. FINITE ELEMENT FORMULATION

Brief formulation of the semi-analytical shell element used here, which was developed recently by Cagdas [15], is given next. In this study, this shell element is modified for free vibration and FPF analyses. The finite element is based on the following displacement field;

$$
\begin{Bmatrix} u_r \\ u_\theta \\ u_z \\ V_{\alpha i} \\ V_{\theta i} \end{Bmatrix} = \sum_{n=0}^{m} \begin{bmatrix} c_n & 0 & 0 & 0 & 0 \\ 0 & s_n & 0 & 0 & 0 \\ 0 & 0 & c_n & 0 & 0 \\ 0 & 0 & 0 & c_n & 0 \\ 0 & 0 & 0 & 0 & s_n \end{bmatrix} \begin{Bmatrix} u_r^n \\ u_\theta^n \\ u_z^n \\ V_{\alpha i}^n \\ V_{\theta i}^n \end{Bmatrix} \quad (1)
$$

where c_n, s_n, and m denote $\cos(n\theta)$, $\sin(n\theta)$, and the total number of harmonics, respectively. u_r^n, u_θ^n, u_z^n, $V_{\alpha i}^n$, and $V_{\theta i}^n$ denote the radial, circumferential, and axial displacement components and the rotations in the nodal coordinate system corresponding to harmonic n, respectively. A local coordinate system (α, θ, z') is defined at a Gauss point on the mid-surface of the cylinder where u, v, and w denote the displacements parallel to α, θ, and z' coordinates and ψ_α, and ψ_θ are the rotations of the transverse normal about θ and α axes. R, R_{ext}, R_{int}, and H denote the mean radius, external radius, internal radius, and thickness respectively.

The cylinder problem considered is schematically shown in Fig. 1 excluding the restraints. The boundary conditions considered are explained in Table 1.
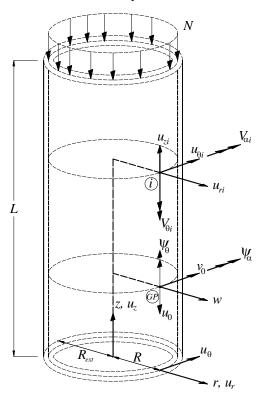

Fig. 1. Details of the cylinder problem and the global and local coordinate systems

Table 1. Boundary conditions considered (F:free, R:restrained) (See Fig. 1)

Name	u_z	u_θ	u_r	V_α	V_θ
S3	F*	R	R	F	R
S4	F*	F	R	F	R
C3	F*	R	R	R	R
C4	F*	F	R	R	R

* u_z is not free at the restrained end

2.1. The Strain-Displacement Relations

The linear and non-linear strain-displacement relations are given below;

$$\varepsilon_\alpha = \varepsilon_{0\alpha} + z' \chi_\alpha \tag{2.1}$$

$$\varepsilon_\theta = \left(\frac{1}{1+z'/R}\right)\left(\varepsilon_{0\theta} + z' \chi_\theta\right) \tag{2.2}$$

$$\gamma_{\alpha\theta} = \varepsilon_{0\alpha\theta} + \left(\frac{1}{1+z'/R}\right)\varepsilon_{0\theta\alpha} + \dots$$
$$z'\left[\left(\frac{1}{1+z'/R}\right)\chi_{\theta\alpha} + \chi_{\alpha\theta}\right] \tag{2.3}$$

$$\gamma_{\theta z'} = \left(\frac{1}{1+z'/R}\right)\left(\gamma_{0\theta z'}\right) \tag{2.4}$$

$$\gamma_{\alpha z'} = \psi_\alpha + w_{0,\alpha} \tag{2.5}$$

$$\varepsilon_{0\alpha}^{nl} = \frac{1}{2}\left[\left(u_{0,\alpha}\right)^2 + \left(v_{0,\alpha}\right)^2 + \left(w_{0,\alpha}\right)^2\right] \tag{2.6}$$

$$\varepsilon_{0\theta}^{nl} = \frac{1}{2R^2}\begin{bmatrix}\left(u_{0,\theta}\right)^2 + \left(v_{0,\theta}\right)^2 + \left(w_{0,\theta}\right)^2 + \dots \\ 2w_0 v_{0,\theta} - 2v_0 w_{0,\theta} + v_0^2 + w_0^2\end{bmatrix} \tag{2.7}$$

$$\varepsilon_{0\alpha\theta}^{nl} = \frac{1}{R}\left(-v_0 w_{0,\alpha} + w_0 v_{0,\alpha}\right) \tag{2.8}$$

$$\varepsilon_{0\theta\alpha}^{nl} = \frac{1}{R}\left(u_{0,\alpha}u_{0,\theta} + v_{0,\alpha}v_{0,\theta} + w_{0,\alpha}w_{0,\theta}\right) \tag{2.9}$$

and,

$$\boldsymbol{\varepsilon}_0 = \begin{Bmatrix}\varepsilon_{0\alpha} \\ \varepsilon_{0\theta} \\ \varepsilon_{0\alpha\theta} \\ \varepsilon_{0\theta\alpha}\end{Bmatrix} = \begin{Bmatrix}\left(u_{0,\alpha}\right) \\ \frac{1}{R}\left(w_0 + v_{0,\theta}\right) \\ \left(v_{0,\alpha}\right) \\ \frac{1}{R}\left(u_{0,\theta}\right)\end{Bmatrix},$$

$$\boldsymbol{\chi} = \begin{Bmatrix}\chi_\alpha \\ \chi_\theta \\ \chi_{\alpha\theta} \\ \chi_{\theta\alpha}\end{Bmatrix} = \begin{Bmatrix}\left(\psi_{\alpha,\alpha}\right) \\ \frac{1}{R}\left(\psi_{\theta,\theta}\right) \\ \left(\psi_{\theta,\alpha}\right) \\ \frac{1}{R}\left(\psi_{\alpha,\theta}\right)\end{Bmatrix},$$

$$\boldsymbol{\varphi} = \begin{Bmatrix}\gamma_{0\alpha z'} \\ \gamma_{0\theta z'}\end{Bmatrix} = \begin{Bmatrix}\psi_\alpha + w_{0,\alpha} \\ \frac{w_{0,\theta}}{R} - \frac{v_0}{R} + \psi_\theta\end{Bmatrix}.$$

2.2. The force and Moment Resultants

The force and moment resultants are given below;

$$\begin{Bmatrix}N_\alpha \\ N_\theta \\ N_{\alpha\theta} \\ N_{\theta\alpha}\end{Bmatrix} = \begin{bmatrix}\overline{A}_{11} & A_{12} & \overline{A}_{16} & A_{16} \\ A_{12} & \hat{A}_{22} & A_{26} & \hat{A}_{26} \\ \overline{A}_{16} & A_{26} & \overline{A}_{66} & A_{66} \\ A_{16} & \hat{A}_{26} & A_{66} & \hat{A}_{66}\end{bmatrix}\begin{Bmatrix}\varepsilon_{0\alpha} \\ \varepsilon_{0\theta} \\ \varepsilon_{0\alpha\theta} \\ \varepsilon_{0\theta\alpha}\end{Bmatrix} + \dots$$
$$\begin{bmatrix}\overline{B}_{11} & B_{12} & \overline{B}_{16} & B_{16} \\ B_{12} & \hat{B}_{22} & B_{26} & \hat{B}_{26} \\ \overline{B}_{16} & B_{26} & \overline{B}_{66} & B_{66} \\ B_{16} & \hat{B}_{26} & B_{66} & \hat{B}_{66}\end{bmatrix}\begin{Bmatrix}\chi_\alpha \\ \chi_\theta \\ \chi_{\alpha\theta} \\ \chi_{\theta\alpha}\end{Bmatrix} \tag{3.1}$$

$$\begin{Bmatrix}M_\alpha \\ M_\theta \\ M_{\alpha\theta} \\ M_{\theta\alpha}\end{Bmatrix} = \begin{bmatrix}\overline{B}_{11} & B_{12} & \overline{B}_{16} & B_{16} \\ B_{12} & \hat{B}_{22} & B_{26} & \hat{B}_{26} \\ \overline{B}_{16} & B_{26} & \overline{B}_{66} & B_{66} \\ B_{16} & \hat{B}_{26} & B_{66} & \hat{B}_{66}\end{bmatrix}\begin{Bmatrix}\varepsilon_{0\alpha} \\ \varepsilon_{0\theta} \\ \varepsilon_{0\alpha\theta} \\ \varepsilon_{0\theta\alpha}\end{Bmatrix} + \dots$$
$$\begin{bmatrix}\overline{D}_{11} & D_{12} & \overline{D}_{16} & D_{16} \\ D_{12} & \hat{D}_{22} & D_{26} & \hat{D}_{26} \\ \overline{D}_{16} & D_{26} & \overline{D}_{66} & D_{66} \\ D_{16} & \hat{D}_{26} & D_{66} & \hat{D}_{66}\end{bmatrix}\begin{Bmatrix}\chi_\alpha \\ \chi_\theta \\ \chi_{\alpha\theta} \\ \chi_{\theta\alpha}\end{Bmatrix} \tag{3.2}$$

$$\begin{Bmatrix}Q_\alpha \\ Q_\theta\end{Bmatrix} = \frac{5}{6}\begin{bmatrix}\overline{A}_{55} & A_{45} \\ A_{45} & \hat{A}_{44}\end{bmatrix}\begin{Bmatrix}\gamma_{\alpha z'} \\ \gamma_{0\theta z'}\end{Bmatrix} \tag{3.3}$$

The rigidity terms appearing in Equations (3.1, 3.2, and 3.3) were presented by Qatu [14]. The lamination angle is taken as the angle between the fiber direction and the local α axis.

2.3. The Element Matrices

The strain energy U_e of element e can be written as

$$U_e = \frac{1}{2}\int_A \left(\mathbf{N}^T \boldsymbol{\varepsilon}^0 + \mathbf{M}^T \boldsymbol{\chi} + \mathbf{Q}^T \boldsymbol{\varphi}\right) dA \tag{4}$$

where $\mathbf{N} = \overline{\mathbf{A}}\boldsymbol{\varepsilon}^0 + \overline{\mathbf{B}}\boldsymbol{\chi}$, $\mathbf{M} = \overline{\mathbf{B}}\boldsymbol{\varepsilon}^0 + \overline{\mathbf{D}}\boldsymbol{\chi}$, and $\mathbf{Q} = \overline{\mathbf{C}}\boldsymbol{\varphi}$ are defined in Equations (3.1, 3.2, and 3.3) and the element stiffness matrix is given below in Eq. (5)

$$\mathbf{K}_e^n = k\pi \int_{-1}^1 \begin{pmatrix}\mathbf{B}_\chi^T \overline{\mathbf{D}}\mathbf{B}_\chi + \mathbf{B}_\varepsilon^T \overline{\mathbf{B}}\mathbf{B}_\chi + \dots \\ \mathbf{B}_\phi^T \overline{\mathbf{C}}\mathbf{B}_\phi + \mathbf{B}_\varepsilon^T \overline{\mathbf{A}}\mathbf{B}_\varepsilon + \dots \\ \mathbf{B}_\chi^T \overline{\mathbf{B}}\mathbf{B}_\varepsilon\end{pmatrix}^n \left(-z_{,\xi}\right) R \, d\xi \tag{5}$$

where, $k = 2$ for $n = 0$, and $k = 1$ for $n = 1,\dots,m$. $\mathbf{B}_\varepsilon$, $\mathbf{B}_\chi$, $\mathbf{B}_\phi$ are the strain-displacement matrices, and the superscript n stands for the nth harmonic. ξ denotes the shape function coordinate.

The kinetic energy of the shell can be expressed as

$$T = \frac{1}{2} \iint_{\alpha \theta} \begin{bmatrix} \left(\dot{u}_0^2 + \dot{v}_0^2 + \dot{w}_0^2\right)\left(I_1 + I_2 \frac{1}{R}\right) + \ldots \\ \left(\dot{\psi}_\alpha^2 + \dot{\psi}_\theta^2\right)\left(I_3 + I_4 \frac{1}{R}\right) + \ldots \\ \left(\dot{u}_0 \dot{\psi}_\alpha + \dot{v}_0 \dot{\psi}_\theta\right)\left(I_2 + I_3 \frac{1}{R}\right) \end{bmatrix} R d\alpha d\theta \qquad (6)$$

where $\{I_1, I_2, I_3, I_4\} = \sum_{k=1}^{NL} \rho^k \{1, z, z^2, z^3\}$ and ρ^k is the

mass density of the kth layer of the cylinder per unit mid-surface area; see Qatu [14]. Similarly, the element mass matrix denoted by $\mathbf{M}^{e,n}$ can be obtained.

The element geometric stiffness matrix is defined in Eq. (7)

$$\mathbf{K}_G^{e,n} = k\pi \int_{-1}^{1} \left(\mathbf{G}^T \mathbf{S} \mathbf{G}\right)^n \left(-z_{,\xi}\right) R d\xi \qquad (7)$$

where $\mathbf{S}$ is a matrix of membrane stresses and $\mathbf{G}$ is a vector of derivatives of in-plane deformations at a Gauss point.

2.4. Free Vibration Analysis of the Axially Compressed Structure

Before conducting the free vibration analysis of the prestressed (axially compressed) structure, the corresponding buckling load should be calculated. First, the pre-buckling deformations under given axial compressive load should be calculated. Then, the buckling load parameter can be obtained by solving the eigenvalue problem given in Eq.(8)

$$\det\left(\mathbf{K}^{n_1} - \lambda_{cr} \mathbf{K}_G^{n_1}\right) = 0 \qquad (8)$$

where $\mathbf{K}^{n_1}$ is the global stiffness matrix, $\mathbf{K}_G^{n_1}$ is the global geometric stiffness matrix corresponding to the harmonic n_1. The critical value of n_1 and the corresponding buckling load, which is equal to $P_{cr} = P_0 \lambda_{cr}$, are determined by trial.

The natural frequency of vibration of a cylinder under a pre-determined level of axial compressive load can be obtained by solving the eigenvalue problem given in Eq.(9)

$$\det\left[\mathbf{K}^{n_2} - f \times \lambda_{cr}\left(\mathbf{K}_G^{n_2}\right) + \left(\omega^{n_2}\right)^2 \mathbf{M}^{n_2}\right] = 0 \qquad (9)$$

where, ω^{n_2} is the circular vibration frequency and $\mathbf{M}^{n_2}$ is the global mass matrix corresponding to the harmonic n_2. The multiplier f is a positive real number, which scales the axial compressive load level. In the present study it is assumed that, $0 \leq f \leq 0.95$. Buckling will generally not be the dominant failure mode for relatively thick cylinders; i.e. cylinders will fail due to excessive stress before buckling. Therefore, first-ply failure analysis using the maximum stress failure criterion is also conducted after obtaining the buckling load. If the FPF

load is less than the buckling load, then the axial load level is kept below the FPF load.

3. VERIFICATION PROBLEMS

The finite element used here has been verified for linear static and stability analyses by Cagdas and Adali [16], and Cagdas [15] and therefore verification problems are only presented for vibration and FPF analyses as given in the following sections.

The non-dimensional in-plane load parameter $\overline{N}$ and the non-dimensional circular frequency Ω are defined as

$$\overline{N} = \frac{10^6 NR}{E_1 LH}, \qquad \Omega = \omega R \sqrt{\rho/E_1} \qquad (10)$$

where, E_1 is the modulus of elasticity in the fiber direction.

3.1. Verification of the Element for Free Vibration Analysis

The problem considered here has been examined by Qatu [14], who has presented exact solutions for open cylindrical shells having two opposite edges simply supported. This type of boundary condition is also referred to in the literature as "all edges simply supported with shear diaphragm boundaries" or S3 type boundary condition as explained in Table 1; Khdeir et al. [2]. To be able to compare the numerical results with the reference analytical results and to prevent numerical problems, u_z is restrained only at the mid-length in the finite element model and not at the cylinder ends. The "shear-diaphragm" compatible boundary conditions used in this study are shown in Fig.2.

Free vibration frequencies of cross-ply laminated cylinders made up of a graphite-epoxy material with

$E_1 = 20.02 \times 10^6 \, psi$, $E_2 = 1.3 \times 10^6 \, psi$,

$G_{12} = 1.03 \times 10^6 \, psi$, $v_{12} = 0.3$

are listed in Table1 in comparison with the results presented by Qatu [14]. For the results presented in Table 1, R/H=100 and stacking sequence is [90°/0°]. The L/R ratio varies between 0.5 and 8. A total of 50 elements are used in the finite element model.
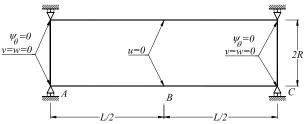

Fig. 2. The "shear-diaphragm" compatible boundary conditions

Excellent agreement with the analytical results of Qatu [14] can be observed from Table 2. It can also be observed that the accuracies of the numerical results do

Table 2. Frequency parameters Ω for R/H=100, [90°/0°] cylinders (material 1).

n	L/R =8 Present Study	Qatu [14]	L/R =4 Present Study	Qatu [14]	L/R =2 Present Study	Qatu [14]	L/R =1 Present Study	Qatu [14]	L/R =0.5 Present Study	Qatu [14]
0	0.08907	0.08907	0.17815	0.17815	0.35629	0.35629	0.73575	0.71259	0.73078	0.73090
1	0.04925	0.04925	0.11653	0.11653	0.24079	0.24079	0.44337	0.44339	0.63562	0.63573
2	0.02182	0.02182	0.06276	0.06276	0.14667	0.14668	0.29320	0.29322	0.49547	0.49559
3	**0.01553**	**0.01553**	0.03836	0.03836	0.09770	0.09770	0.21023	0.21025	0.38987	0.38999
4	0.02143	0.02143	**0.03146**	**0.03147**	0.07183	0.07184	0.16103	0.16105	0.31682	0.31694
5	0.03296	0.03298	0.03697	0.03699	**0.06124**	**0.06126**	0.13133	0.13136	0.26676	0.26689
6	0.04785	0.04789	0.04971	0.04975	0.06308	0.06312	0.11555	0.11560	0.23332	0.23335
7	0.06562	0.06570	0.06669	0.06678	0.07425	0.07433	**0.11152**	**0.11160**	0.21256	0.21273
8	0.08618	0.08632	0.08692	0.08707	0.09162	0.09177	0.11763	0.11777	**0.20288**	**0.20311**
9	0.10948	0.10971	0.11007	0.11030	0.11336	0.11359	0.13192	0.13216	0.20295	0.20327
10	0.13552	0.13587	0.13602	0.13637	0.13856	0.13892	0.15247	0.15284	0.21162	0.21208

not significantly detoriate with increasing mode number *n*. This probably is because the number of elements used was relatively high for the problem under consideration.

3.2. Verification of the element for FPF analysis

FPF analysis of a R/H=60, L/R =1, composite cylinder made up of T300/5208 material under axial compression is considered next. The S3 boundary conditions are imposed. The properties of T300/5208 graphite/epoxy pre-preg are listed in Table 3, see Ochoa and Reddy [20]. The numerical results obtained using the axisymmetric

Table 3. Material properties of T300/5208 graphite/epoxy pre-preg. (units: N-mm)

E_1	132379.37	X_T	1513.40
E_2	10755.82	X_C	1696.11
E_3	10755.82	$Y_T = Z_T$	43.78
$G_{12} = G_{13}$	5653.70	$Y_C = Z_C$	43.78
G_{23}	3378.43	R	67.57
$\nu_{12} = \nu_{13}$	0.24	$S = T$	86.87
ν_{23}	0.49		

shell element are given in Table 4, in comparison with the results obtained using a 2D shell element; Cagdas and Adali [16]. For both models, stresses are extrapolated from the Gauss points to the element corner nodes. As can be seen from Table 4 the maximum difference between the 2D shell element results and the axisymmetric shell element results is less than **3%** for all of the cases considered. A refined mesh is required to

obtain plausible FPF analysis results using the 2D shell elements. However, it should be noted that, excessive mesh refinement may result in errors when using the 2D shell element. It is observed that, if, due to mesh refinement, the thickness of the 2D shell element becomes less than ¼ of the element's shorter edge length a finer mesh may yield unreliable results. The axisymmetric element does not demonstrate such behavior.

Table 4. FPF load parameters $\overline{N}_{FPF}$ for R/H=60, L/R =1, S3 B.C., material T300/5208.

Lay-up	Axisym.(50 el.)	2D (32×10)
[90/90]s	112465	115469
[0/0]s	3482472	3394267
[90/0]s	756430	767994
[0/90]s	812289	814023

3.3. Verification of the element for free vibration analysis including axial stress

Before proceeding with the numerical study, the numerical results presented by Greenberg and Stavsky [10] for two layered cross-ply laminated composite cylinders under 10⁴lbs/in. axial compressive force with S3 B.C. are compared with the results obtained in this study; see Table 5. Note that, the inner layer has fibers aligned in circumferential direction with a thickness of 4 mm and the total thickness is equal to 10 mm. The material properties used by Greenberg and Stavsky [10] are; $E_1 = 19 \times 10^9 \, N/m^2$, $E_2 = 7.6 \times 10^9 \, N/m^2$

Table 5. Free vibration frequencies $\omega(n)/10^3$ (sec⁻¹) for R/H=20, S3 B.C.

L/R	Donnel theory [10]	Love-type Theory [10]	Greenberg and Stavsky [10]	Present Study
.5	16.05 (4)	15.39 (4)	10.40 (4)	9.61 (4)
.9	9.02 (4)	8.45 (3)	6.51 (4)	5.96 (4)
2	4.86 (3)	4.33 (3)	3.96 (3)	3.27 (3)
4	2.92 (4)	2.41 (2)	2.65 (2)	2.04 (2)

Table 6. Frequency parameters Ω for R/H=60, [90°/0°]$_s$, L/R =1 cylinder.

$.n_2$	f =0.00	f =0.25	f =0.50	f =0.75	f =0.80	f =0.90	f =0.95
0	0.6492	0.6487	0.6459	0.6426	0.6406	0.6382	0.6319
1	0.4134	0.4125	0.4080	0.4029	0.3996	0.3959	0.3938
2	0.2714	0.2701	0.2632	0.2551	0.2499	0.2439	0.2406
3	0.1980	0.1962	0.1867	0.1751	0.1674	0.1583	0.1531
4	0.1645	0.1623	0.1506	0.1360	0.1259	0.1135	0.1062
5	**0.1626**	**0.1605**	**0.1486**	**0.1338**	**0.1236**	**0.1109**	**0.1033**
6	0.1876	0.1858	0.1756	0.1632	0.1550	0.1419	0.1173
7	0.2324	0.2309	0.2228	0.2132	0.2069	0.1819	0.1462
8	0.2913	0.2901	0.2837	0.2762	0.2690	0.2439	0.2121
9	0.3610	0.3600	0.3549	0.3489	0.3410	0.3188	0.2951
10	0.4398	0.4390	0.4348	0.4300	0.4230	0.4051	0.3868

Table 7. Frequency parameters Ω for R/H=60, [90°/0°]$_s$, L/R =10 cylinder.

$.n_2$	f =0.00	f =0.25	f =0.50	f =0.75	f =0.80	f =0.90	f =0.95
0	0.0649	0.0648	0.0646	0.0642	0.0641	0.0638	0.0637
1	0.0380	0.0379	0.0374	0.0367	0.0365	0.0361	0.0358
2	**0.0222**	**0.0219**	**0.0211**	**0.0197**	**0.0193**	**0.0185**	**0.0180**
3	0.0358	0.0357	0.0352	0.0342	0.0340	0.0334	0.0331
4	0.0660	0.0659	0.0656	0.0648	0.0644	0.0633	0.0624
5	0.1059	0.1059	0.1057	0.1043	0.1036	0.1010	0.0984
6	0.1547	0.1546	0.1547	0.1522	0.1509	0.1402	0.1130
7	0.2118	0.2118	0.2136	0.2084	0.2298	0.1794	0.1455
8	0.2771	0.2771	0.2788	0.2808	0.2857	0.2404	0.2125
9	0.3504	0.3504	0.3522	0.4045	0.3972	0.3171	0.2954
10	0.4312	0.4312	0.4327	0.4510	0.4528	0.4037	0.3870

$G_{12} = 4.1 \times 10^9 \, N/m^2$, $G_{13} = 19 \times 10^6 \, N/m^2$,

$G_{23} = 19 \times 10^6 \, N/m^2$, $\rho = 1.643 \times 10^3 \, kg/m^3$, $v_{12} = 0.3$.

As can be observed from Table 5, there are considerable differences between different shell theories and the results obtained in this study are lower than the results presented by Greenberg and Stavsky [10], even though shear deformation was considered in [10]. The differences may be attributed to the influence of thickness coordinate/radius ratio considered in the present study.

4. NUMERICAL RESULTS AND DISCUSSION

The problem under consideration is the determination of the free vibration frequencies of cross-ply laminated cylinders under pre-determined levels of axial compressive load. The axial compressive load is limited to the corresponding critical buckling load or to the FPF load of the cross-ply cylinder analyzed.

4.1. Numerical Results

In the following sub-sections the numerical results obtained using 50 axisymmetric finite elements for the selected problems are given both in tabular and graphical forms. The material used is specified as T300/5208

graphite-epoxy for which material properties are given in Table 3. The non-dimensional thicknesses of the 0° and 90° plies are given by $h_0 = H_0 / H$ and $h_{90} = H_{90} / H$, respectively, where H_0 and H_{90} are the thicknesses of 0° and 90° plies.

4.1.1. The influence of L/R ratio

In Table 6, numerical results are presented for S3 B.C., h_{90} =0.25, L/R=1 and $H=R/60$ and for several values of f=[0,0.95]. The non-dimensional buckling load $\bar{N}_{cr}$ =713160, and the corresponding critical wave number n_{cr}=6 and $\bar{N}_{FPF}$ =756430 (see Table 3) for this case.

As can be observed from Table 6, for the non-compressed case, i.e. for f=0, the 5th harmonic gives Ω_{min} =0.1626, which is the lowest vibration frequency and Ω values decrease with increasing f for all of the n_2 values considered. Also, the value of $n_{2,min}$ does not change for $f \leq 0.95$ and the numerical results show that

there is a smooth decrease up to f=0.9 and a sharp decrease after higher axial compressive load level is reached. This sudden change is a warning of buckling and may be helpful while inspecting or monitoring related structures. Another observation that can be made from
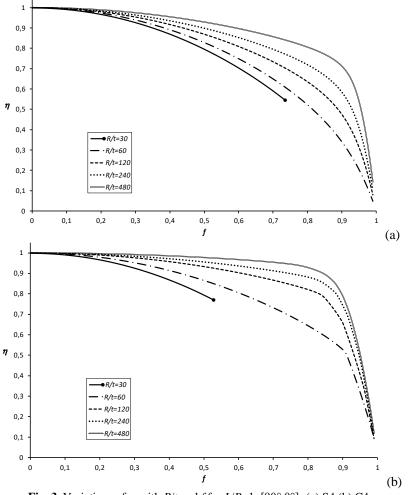
Fig. 3. Variations of η with R/t and f for L/R=1, [90°,0°]$_s$ (a) S4 (b) C4

Table 6 is that, the negative influence of axial compression on the free vibration frequency is very high for some n_2 values, especially for the ones corresponding to the lowest natural frequency and the buckling mode shape. Here, for the cases considered, f=0.75 leads to a reduction of around 20% in Ω_{min} and the other frequency values are reduced less. The decrease in Ω with increasing f is more pronounced for n_2=5 and 6. These preliminary results obtained show that the negative influence of axial compression on the free vibration behavior will be lower if appropriate safety factors are used against buckling.

Numerical results are also presented in Table 7 for L/R =10, in order to investigate the influence of cylinder L/R ratio. For this case, $\overline{N}_{cr}$ =88740, n_{cr}=6 and $\overline{N}_{FPF}$ =106266. It can be observed from Table 7 that, for L/R =10, the negative influence of axial compression is lower comparing with the case L/R =1.

4.1.2. Buckling and FPF critical cylinders
The percentage difference denoted by η is defined as

$$\eta^n = \frac{\left(\Omega^{n,f=0} - \Omega^{n,f\neq0}\right)}{\Omega^{n,f=0}} \times 100$$

where $\Omega^{n,f\neq0}$, $\Omega^{n,f=0}$ denote the nth vibration mode non-dimensional frequencies corresponding to the cases $f \neq 0$ and $f = 0$.

It can be observed from Figures 3(a) and 3(b) that, the influence of axial compression on the free vibration frequencies is higher for thicker cylinders and thicker cylinders more rapidly loose rigidity with increasing axial compression level comparing with thinner cylinders especially for f<0.8. The curvature of the η curve changes rapidly for f>0.8 and the behavior is only slightly different for S4 and C4 boundary conditions. It can also be observed that the decrease in omega with increasing f is unexpectedly lower for thinner cylinders.

The results obtained, in general, show that it may not be possible to correlate free vibration and buckling parameters. Different boundary conditions are also considered and the vibration frequency-buckling load correlation is shown to be related with the boundary conditions. However, it is influence is found out to be limited. However, as expected cylinders with C4 BC are more stiff comparing with the cylinders with S4 BC.

4. CONCLUSIONS

A finite element formulation for free vibration analysis of axially compressed, moderately thick, cross-ply laminated composite cylinders is presented. Firstly, some verification problems are solved and the high accuracy of the element in free vibration and FPF analyses is demonstrated. The free vibration frequencies obtained for the non-compressed cases are found out to be in excellent agreement with the analytical results found in the literature. Then, the effects of the axial compression, geometry, end conditions, and the stacking sequence on the free vibration frequencies are investigated.Numerical results for free vibration analyses are presented for axially compressed cylinders having different boundary conditions and for which the level of axial compression is kept below the corresponding linear buckling and the first ply failure loads. The numerical results show that, the related natural frequencies decrease somewhat linearly with increasing axial compressive load levels up to about 70~80% of the buckling loads of the structures considered and decrease non-linearly for higher load levels. Therefore, it is deduced that, it may, in practical applications, be possible to predict the onset of buckling by monitoring the change of the natural frequencies under increasing axial compressive load levels. It is also revealed that the decrease in frequency parameters is more pronounced for the mode shapes corresponding to the lowest frequency, i.e. not for the ones corresponding to the buckling mode shapes.

The most important outcome of this study for design purposes is that, the negative influence of axial compression is found out to be the reduction of the minimum natural frequency by about 20% even for f=0.75. Also, it is revealed that higher L/R ratios lead to lower reduction and for thick cylinders, for which the buckling load is lower than the FPF load, the reduction in free vibration frequency will be much lower.

REFERENCES

[1] Qatu, Mohamad S. "Recent research advances in the dynamic behavior of shells: 1989-2000, Part 1: Laminated composite shells", *Applied Mechanics Reviews*, 55(4): 325-350, (2002).

[2] Khdeir, A. A., J. N. Reddy, and D. Frederick. "A study of bending, vibration and buckling of cross-ply circular cylindrical shells with various shell theories", *International Journal of Engineering Science*, 27(11): 1337-1351, (1989).

[3] Jones, Robert M., and Harold S. Morgan. "Buckling and vibration of cross-ply laminated circular cylindrical shells", *AIAA Journal*, 13(5): 664-671, (1975).

[4] Armenàkas, Anthony E. "Influence of initial stress on the vibrations of simply supported circular cylindrical shells", *AIAA Journal*, 2(9): 1607-1612, (1964).

[5] Rosen, Aviv, and Josef Singer. "Vibrations of axially loaded stiffened cylindrical shells", *Journal of Sound and Vibration*, 34(3): 357-IN3, (1974).

[6] Bradford, L. G., and S. B. Dong. "Natural vibrations of orthotropic cylinders under initial stress", *Journal of Sound and Vibration*, 60(2): 157-175, (1978).

[7] Greenberg, J. B., and Y. Stavsky. "Vibrations of axially compressed laminated orthotropic cylindrical shells, including transverse shear deformation", *Acta Mechanica*, 37(1-2) : 13-28, (1980).

[8] Yamada, Gen, Toshihiro Irie, and Mitsuo Tsushima. "Vibration and stability of orthotropic circular cylindrical shells subjected to axial load", *The Journal of the Acoustical Society of America*, 75(3): 842-848, (1984).

[9] Chang, Jeng-Shian, and Chen-Hong Lin. "Buckling and free vibration of cross-ply laminated circular cylindrical shells subjected to axial thrust and lateral pressure loading according to a higher order displacement field", *Thin-Walled Structures*, 13(3): 177-196, (1992).

[10] Greenberg, J. B., and Y. Stavsky. "Vibrations and buckling of composite orthotropic cylindrical shells with nonuniform axial loads", *Composites Part B: Engineering*, 29(6): 695-70, (1998).

[11] Matsunaga, H. "Free vibration of thick circular cylindrical shells subjected to axial stresses", *Journal of Sound and Vibration*, 211(1): 1-17, (1998).

[12] Skukis, E., K. Kalnins, and A. Chate. "Preliminary assessment of correlation between vibrations and buckling load of stainless steel cylinders", Shell Structures Theory and Applications, CRC Press, London, (2013).

[13] Arbelo, Mariano A., et al. "Vibration correlation technique for the estimation of real boundary conditions and buckling load of unstiffened plates and cylindrical shells", *Thin-Walled Structures*, 79: 119-128, (2014).

[14] Qatu, Mohamad S. "Accurate equations for laminated composite deep thick shells", *International Journal of Solids and Structures*, 36(19) : 2917-2941, (1999).

[15] Cagdas, Izzet U. "Stability analysis of cross-ply laminated shells of revolution using a curved axisymmetric shell finite element.", *Thin-Walled Structures*, 49(6): 732-742, (2011)

[16] Cagdas, Izzet U., and Sarp Adali. "Buckling of cross-ply cylinders under hydrostatic pressure considering pressure stiffness*", Ocean engineering*, 38(4) : 559-569, (2011).

[17] Cagdas, Izzet U. "Optimal design of filament wound truncated cones under axial compression." *Composite Structures*, 170: 250-260, (2017)

[18] Cagdas, Izzet U. "Optimal design of variable stiffness laminated composite truncated cones under lateral external pressure", *Ocean Engineering*, 145: 268-276, (2017)

[19] Cagdas, Izzet U., and Sarp Adali. "Effect of Fiber Orientation on Buckling and First-Ply Failures of Cylindrical Shear-Deformable Laminates", *Journal of Engineering Mechanics*, 139(8) : 967-978, (2013).

[20] Ochoa, Ozden O., and Junuthula Narasimha Reddy. "Finite element analysis of composite laminates", Springer, Dordrecht, (1992).